The International Journal of Advanced Manufacturing Technology (2023) 129:1127–1143
https://doi.org/10.1007/s00170-023-12332-x

ORIGINAL ARTICLE

Relationship between surface characteristics and the fatigue life of deep rolled AISI 4140 steel

Augusto Moura Martins[1] · Diogo Azevedo de Oliveira[1] · Frederico de Castro Magalhães[1] · Alexandre Mendes Abrão[1]

Received: 11 April 2023 / Accepted: 12 September 2023 / Published online: 26 September 2023

Abstract
Deep rolling is an effective and economically viable mechanical surface treatment that induces surface deformation by the action of a rolling tool. It is capable of reducing roughness, increasing hardness, and inducing compressive residual stresses on the workpiece surface, thus increasing the fatigue strength of the component. This behavior, however, is only achieved with use of suitable parameters. This work investigates the surface characteristics and fatigue life of hardened AISI 4140 steel subjected to turning followed by deep rolling under distinct conditions. The findings indicates that for the turned samples, roughness increases with turning feed rate, resulting in fatigue life reduction. Deep rolling promotes a reduction in surface roughness, promotes surface deformation, and causes an increase in both surface hardness and fatigue life. Surprisingly, the samples with the highest surface roughness after turning achieved the longest fatigue lives after deep rolling. The areal power spectral density analysis of the surface topography was able to identify distinct effects of deep rolling for each level of pressure used. The morphology analysis indicates an initial loss of orientation, followed by the creation of a new orientation after deep rolling under high pressures. Furthermore, the interaction between deep rolling feed and deep rolling pressure presents a significant effect on the roughness parameters, indicating that different behaviors depend on each parameter level used. Deep rolling also affects the form of the fatigue fracture, reducing the number of nucleation sites, and modifying the final overload fracture site.

Keywords Turning · Deep rolling · Surface topography · Roughness · Hardness, Fatigue life · AISI 4140 steel

1 Introduction

Surface treatments can fall in the following categories: coatings, thermal, thermochemical, and mechanical treatments. Mechanical treatments plastically deform the material surface, producing work hardening and inducing compressive residual stresses. One of the most employed mechanical treatments is deep rolling [1]. In deep rolling, a tool with a specific geometry (ball or roller) and high stiffness compresses the work material surface, plastically deforming the roughness peaks generated during the previous machining operation [2]. Similar to other manufacturing processes, deep rolling has several parameters to be controlled: force (or pressure), feed, speed, tool geometry and material, contact conditions, and number of passes [3], among which force is the most important [4]. In addition to these parameters, the final surface condition is expected to be influenced by the previous machining operations, with roughness after deep rolling having a direct relationship with roughness before deep rolling [5]. A reduction in surface roughness after deep rolling was reported by a series of authors. Nalla et al. [6] observed a reduction larger than 50% on Rz after deep rolling Ti-6Al-4 V, and Avilés et al. [7] noticed that the Ra value decreased from 0.68 to 0.12 µm after deep rolling AISI 1045 steel. Prabhu et al. [8] reported significant reduction on the surface roughness of AISI 4140 steel (225 HV) after deep rolling, with a maximum reduction of 95% on the Ra value in comparison with the turned specimens. According to these authors, the higher the deep rolling force, the higher the reduction in surface roughness. A roughness reduction was also observed by Martins et al. [9] after deep rolling hardened AISI 4140 steel (40 HRC), with the Rq

✉ Augusto Moura Martins
augusto.mmartins2@gmail.com

[1] Graduate Program in Mechanical Engineering, Universidade Federal de Minas Gerais, Av. Antônio Carlos, 6627 Campus Pampulha, Belo Horizonte, MG 31270-901, Brazil

value of the deep rolled samples being approximately 4.5% of that of the turned samples. However, Rodríguez et al. [10] noticed an increase in the Rz value when excessive force is applied in deep rolling of AISI 1045 steel. According to these authors, when an excessively high force is used, the rolling element damages the surface and produces a profile with grooves. Klocke and Liermann [11] stated that the rolling feed must be different from that used in the previous machining process to allow deep rolling to correctly deform the roughness peaks. Thus, a feed reduction leads to a decrease in surface roughness [12], owing to the fact that the contact width between the rolling tool and the workpiece becomes much larger than the rolling feed, resulting in an overlap [13]. Denkena et al. [14] proposed the overlap to be calculated using the ratio of the deep rolling feed to the contact width. The results indicated that an increase from 50 to 80% in the overlap promoted a reduction from 1.01 to 0.65 µm in the Rz of AISI 1045 steel samples. In contrast, an increase in deep rolling feed could create a condition where the feed is larger than the width of the contact area between the tool and the work surface, being incapable of improving the surface quality [15].

In addition to the analysis of the well-established roughness amplitude parameters (Ra, Rq, Rz, Rt, etc.), other surface analysis methods (such as power spectral density (PSD)) can be conducted and are capable of detecting distinct characteristics. Among these methods are the PSD analysis [16] and the analysis of surface texture direction using the morphological rose of motifs [17]. The PSD analysis can be extended to a tridimensional surface analysis by the areal power spectral density (APSD) analysis and corresponds to the square of the amplitude of the Fourier transform of the measured topography [18]. APSD can be obtained by a fast Fourier transform (FFT) of the profile along the workpiece length [19]. The spectral density analysis is sensitive to disturbances generated on the surface by machining parameters. It can be employed to identify parameter values, indicating the frequency related to the turning feed [16], detecting tool wear [19], and the presence of machine vibration [20] by noticing distinct frequencies on the spectrum. The morphological rose is generated by computing the density of motifs oriented in a specific direction, identified in relation to an axis in the original sample. The directional properties can affect fluid flow and the ability of the surface to retain lubricant [17]. Both APSD and the morphological rose analyses were applied to burnished surfaces [21] and were able to identify surface property changes, even for surfaces with roughness values (Ra parameter) statistically equivalent.

As previously mentioned, deep rolling can increase the surface hardness and induce compressive residual stresses [2], in addition to reduce the surface roughness [6], features responsible for the enhancement of the fatigue strength. An increase in the fatigue strength of various alloys after deep rolling was reported by a number of authors: Ti-6Al-4 V titanium alloy [6], AISI 304 and 316 austenitic stainless steels [2], AISI 1045 medium carbon steel [7], Al7075 aluminum alloy [12], and AISI 4140 low alloy steel [9]. Prabhu et al. [5] reported that the deep rolling force was the most relevant parameter on the fatigue life of AISI 4140 low alloy steel. According to Muñoz-Cubillos et al. [2], deep rolling is capable of delaying fatigue crack nucleation and reducing fatigue crack propagation, the latter effect being also reported by Nalla et al. [6]. The reduction in the fatigue crack nucleation was associated to the lower number of ratchet marks on the fracture surface of the deep rolled samples, behavior observed on AISI 304 and 316 austenitic stainless steels by Muñoz-Cubillos et al. [2] and on AISI 4140 steel by Martins et al. [9]. Besides altering the number of fatigue nucleation sites, deep rolling was also able to affect the final fracture region. The region with the presence of dimples, indicating ductile overload fracture [7], shifted from the center of the cross-section of turned specimens to a larger area not near the center of the deep rolled samples [9].

Considering the ability of deep rolling to alter surface and subsurface characteristics that affect the fatigue strength of alloys and the influence of the selected parameters on the final result, the aim of this work is to evaluate the influence of turning and deep rolling parameters on the surface topography and hardness, microstructure alterations, fatigue life, and fatigue fracture of hardened AISI 4140 steel. Turning feed, the principal parameter responsible for the machined surface roughness and often neglected when machined components are further subjected to deep rolling, is properly investigated, considering the possible interaction between turning (feed) and deep rolling (pressure and feed) parameters. Finally, the effectiveness of APSD and surface texture directionality analyses in contributing to a more comprehensive assessment of the surface topography is evaluated, considering the application of these approaches to evaluate the influence of anisotropy and directionality in the fatigue behavior.

2 Materials and methods

AISI 4140 steel was selected as work material. After quenching and tempering to reach an average hardness of 40 ± 2 HRC, the specimens were turned in a CNC lathe with power of 5.5 kW and maximum rotational speed of 3500 rpm. Turning was carried out using $TiCNAl_2O_3$-Ti-coated carbide inserts (Mitsubishi Carbide grade UE6110) with ISO geometry VCMT 160408 mounted on an ISO SVVCN 2020-K16N tool-holder from the same manufacturer. The specimens were turned to reach a geometry suitable for performing the fatigue tests using a cutting speed (v_c) of 45 m/min, depth of cut (a_p) of 0.5 mm, and three distinct feed (f)

values (0.10, 0.15, and 0.20 mm/rev). After turning, part of the specimens were deep rolled using an Ecoroll HG6-20 hydrostatic tool (Ø 6.35 mm). Deep rolling was performed with a synthetic fluid at a concentration of 10% in water. A rolling speed of 40 m/min was used and three distinct values of pressure (10, 25, and 20 MPa) and feed (0.06, 0.09, and 0.12 mm/rev) were tested. The experiment steps and parameters used for the manufacturing of the specimens are presented in Fig. 1. Four specimens were manufactured for each parameter combination.

After manufacturing, the surface topography of the specimens was assessed using a Hommelwerke Hommel Etamic T8000 profilometer (diamond stylus with tip angle of 90° and tip radius of 5 µm). The following roughness parameters were measured: arithmetical mean deviation (Ra), maximum profile peak height (Rp), and maximum profile valley depth (Rv). The sum of Rp and Rv represents the maximum height of the profile (Rz). The surface topography was used to conduct the APSD analysis and to generate the morphological roses. Figure 2 shows the region of the specimens selected for the surface topography analysis, where the *X*-axis is parallel to the specimen rotation axis. The *X* direction was selected as it is the same as the manufacturing processes feed direction.

Microstructure analyses were conducted in a Jeol JSM-IT300 scanning electron microscope (SEM) and ultra-microhardness measurements were performed using a Shimadzu DUH-211S ultra-microhardness tester. The load-unload mode was used to perform the measurements with a Berkovich indenter and applying of 200 mN. Rotating bending fatigue tests were undertaken in a Fatigue Dynamics RBF-200 testing machine. The bending moment applied during the tests was equivalent to a stress 870 MPa (65% of the yield stress of AISI 4140 steel hardened to 40 HRC) and rotational speed of 5000 rpm. The number of cycles to failure was recorded for each specimen. After the fatigue tests, the cross-section of selected fractured specimens was observed in a Quanta 200 FEG SEM.

3 Results

3.1 Surface roughness

Figure 3 (with a logarithmic ordinate scale) shows that deep rolling is capable to significantly reduce the arithmetical mean deviation (Ra parameter), regardless of the manufacturing conditions, behavior that has been previously observed [10]. Moreover, deep rolling is able to reduce the influence of the feed used in the previous turning operation, since similar Ra values were obtained after deep rolling for distinct *f* values employed in turning (0.1–0.15 and 0.2 mm/rev). However, increasing turning feed resulted in higher Ra values after deep rolling. Regarding the influence of the deep rolling parameters, it can be observed a tendency of increase in Ra with the deep rolling feed. The combination of the highest deep rolling feed and pressure induced higher roughness values, as observed by Rodríguez et al. [10].

An analysis of variance (with a significance level of 0.05) was conducted and the results indicated that turning feed, deep rolling feed, and deep rolling pressure were statistically significant (contributions of 10.86, 36.20, and 5.36%, respectively), as well as the interaction between deep rolling feed and pressure (contribution of 11.66%).

The main effect and interaction plots for Ra are shown in Fig. 4. Figure 4(a) presents the influence of the turning feed on the Ra parameter. The highest turning feed produced the highest Ra value after deep rolling. The fact that the increase in roughness is not proportional to the turning feed can be related to the ratio of the turning feed to the deep rolling feed. As recommended by Klocke and Liermann [11], the turning and deep rolling feeds should have distinct values. When these values are close ($f = 0.10$ mm/rev and $fr = 0.09$ mm/rev), the ability of deep rolling to deform the roughness peaks is reduced and the decrease in roughness after deep rolling is not maximized. Figure 4(b) shows that the arithmetical mean deviation value increases with

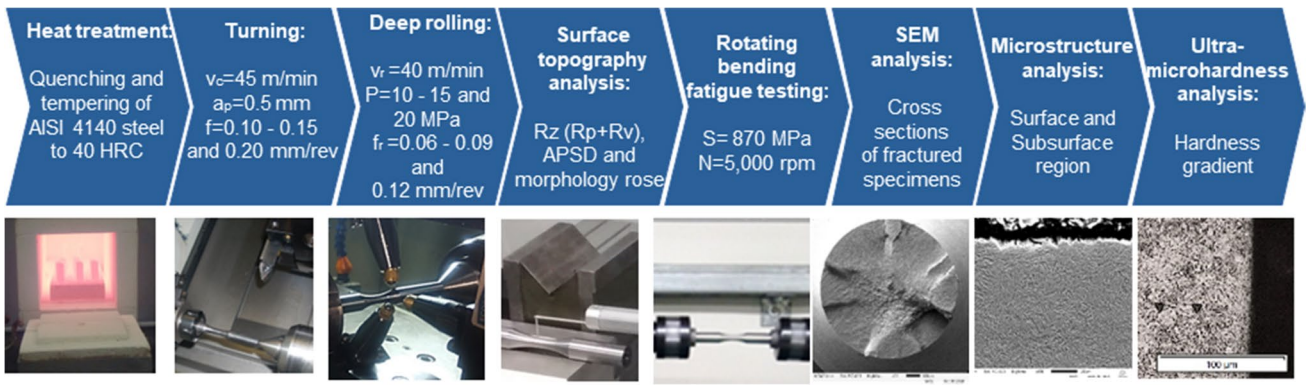

Fig. 1 Schematic diagram of the experimental procedure

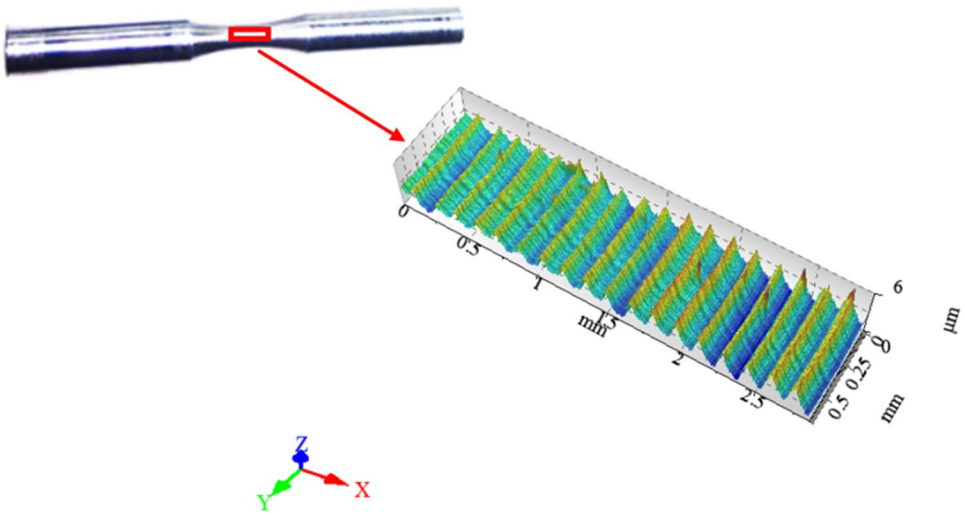

Fig. 2 Surface topography analysis

the elevation of deep rolling feed. Increasing deep rolling feed reduces the overlap and diminishes the intensity of deep rolling, hindering its ability to deform the roughness peaks and convey the material to the valleys, thus impairing the reduction of roughness. Considering the influence of deep rolling pressure presented in Fig. 4(c), an increase in the Ra values is noted with the elevation of this parameter. Higher forces can deform the surface more easily and are capable of generating grooves; therefore, an excessive force can damage the surface finish.

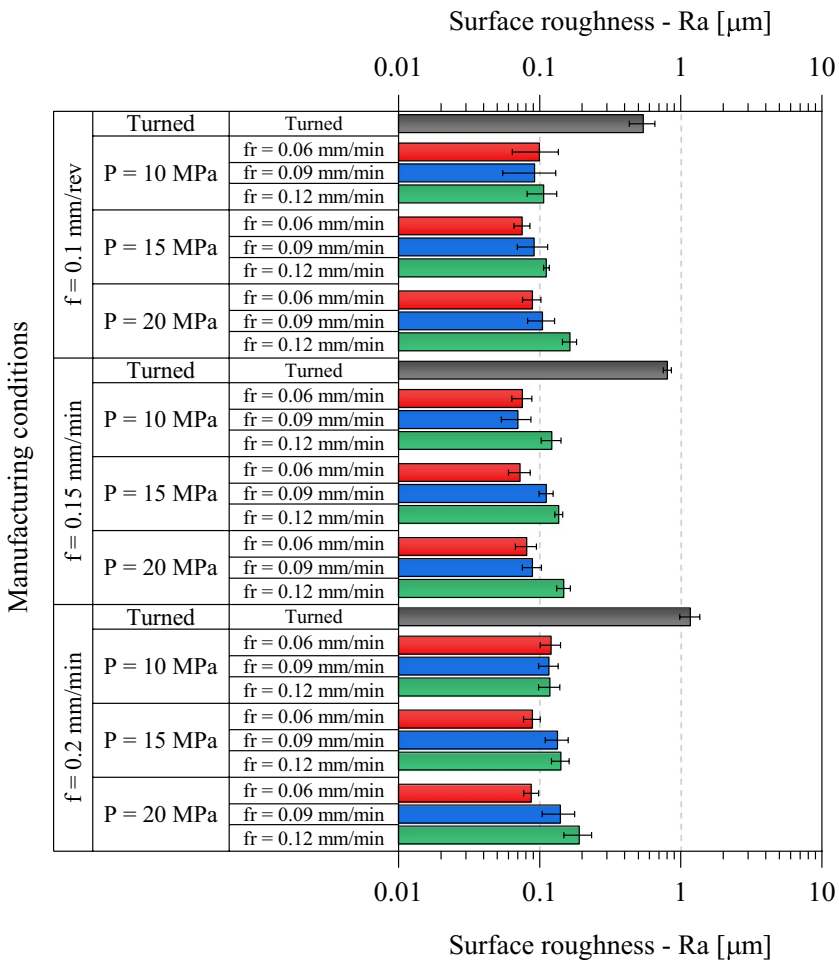

Fig. 3 Effect of the turning feed and deep rolling feed and pressure on the arithmetical mean deviation (Ra parameter) of hardened AISI 4140 steel

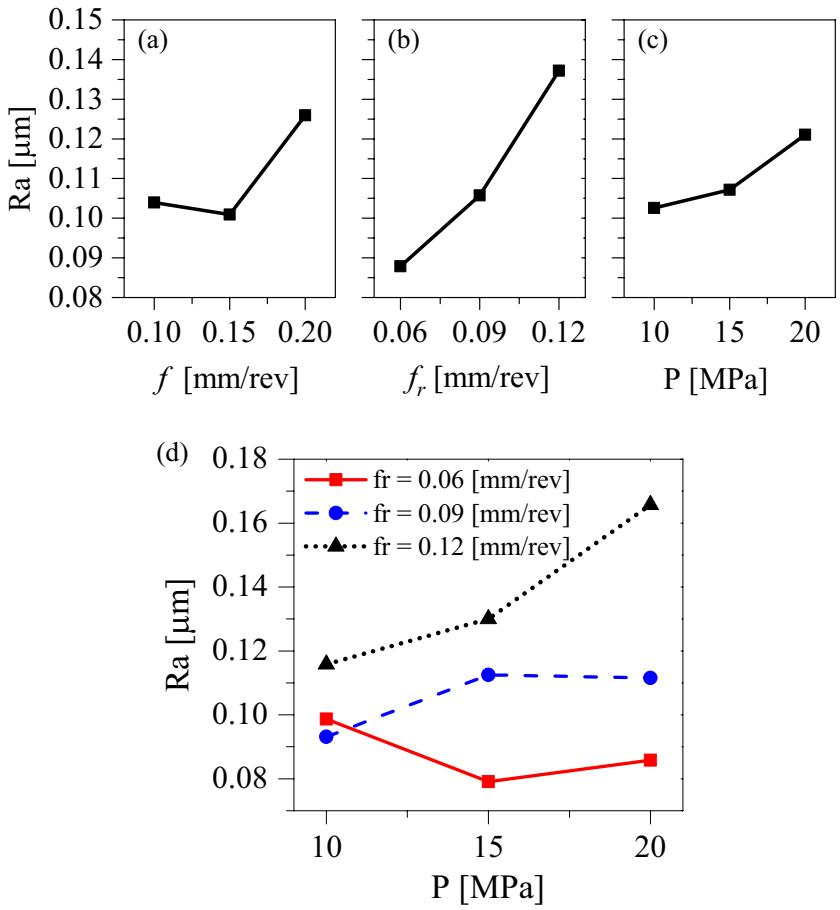

Fig. 4 Effect plots for Ra after turning and deep rolling hardened AISI 4140 steel: (**a**) turning feed, (**b**) deep rolling feed, (**c**) deep rolling pressure, and (**d**) interaction effect plot

The effect of the interaction between deep rolling feed (f_r) and pressure (P) can be observed in Fig. 4(d). The variation in the Ra values with deep rolling feed is affected by deep rolling pressure: higher rolling pressures produce a larger variation in Ra for distinct deep rolling feed values. This behavior can be observed by the increase in the difference between the mean values for Ra under each pressure. Therefore, while surface roughness is not drastically affected by pressure when the lowest and intermediate deep rolling feed values are used, an appreciable increase in Ra is noted when deep rolling with a feed of $f_r = 0.12$ mm/rev.

The maximum height of the profile (Rz) represents the sum of the maximum profile peak height (Rp) and maximum profile valley depth (Rv), which are presented in Fig. 5 for each manufacturing condition. Similar to the Ra results, the ability of deep rolling to reduce the roughness amplitude is evident (see the logarithmic scale used to allow comparisons between the turned samples and those deep rolled under distinct conditions). Moreover, deep rolling alters the contribution of Rp and Rv to Rz: for the turned samples, Rp presents higher amplitude than Rv; however, the ratio of Rp to Rv reduces considerably after deep rolling. Deep rolling deforms the roughness profile, affecting more significantly the value of Rp, probably because the peaks are more easily deformed than the valleys. Regarding the influence of the deep rolling parameters, an increase in the roughness parameters is noticed with the elevation of deep rolling feed. The analysis of variance (significance level of 0.05) for Rp indicates that turning feed, deep rolling feed, and deep rolling pressure are statistically significant with respective contributions of 4.57%, 22.43%, and 12.82%, as well as the interaction between deep rolling feed and pressure (contribution of 7.71%). In the case of Rv, only the turning feed (contribution of 16.25%) and the deep rolling feed (contribution of 49.96%) are statistically significant.

The main effects plots for Rp and Rv are shown in Fig. 6. Figure 6(a) shows that the value of Rp after deep rolling increases with the feed employed in the previous turning operation, though not directly proportional. Again, employing a turning feed of $f = 0.10$ mm/rev and near the lowest deep rolling feed ($fr = 0.09$ mm/rev) allows a condition in which surface peak deformation is impaired [11]. Thus, the lower roughness values after deep rolling are found for the intermediate turning feed ($f = 0.15$ mm/rev). The effect of deep rolling feed (Fig. 6(b)) is analogous to that observed for Ra (the higher the deep rolling feed, the higher the Rp value). When higher deep rolling feeds are used, the overlap is decreased, reducing the roughness peaks deformation [14].

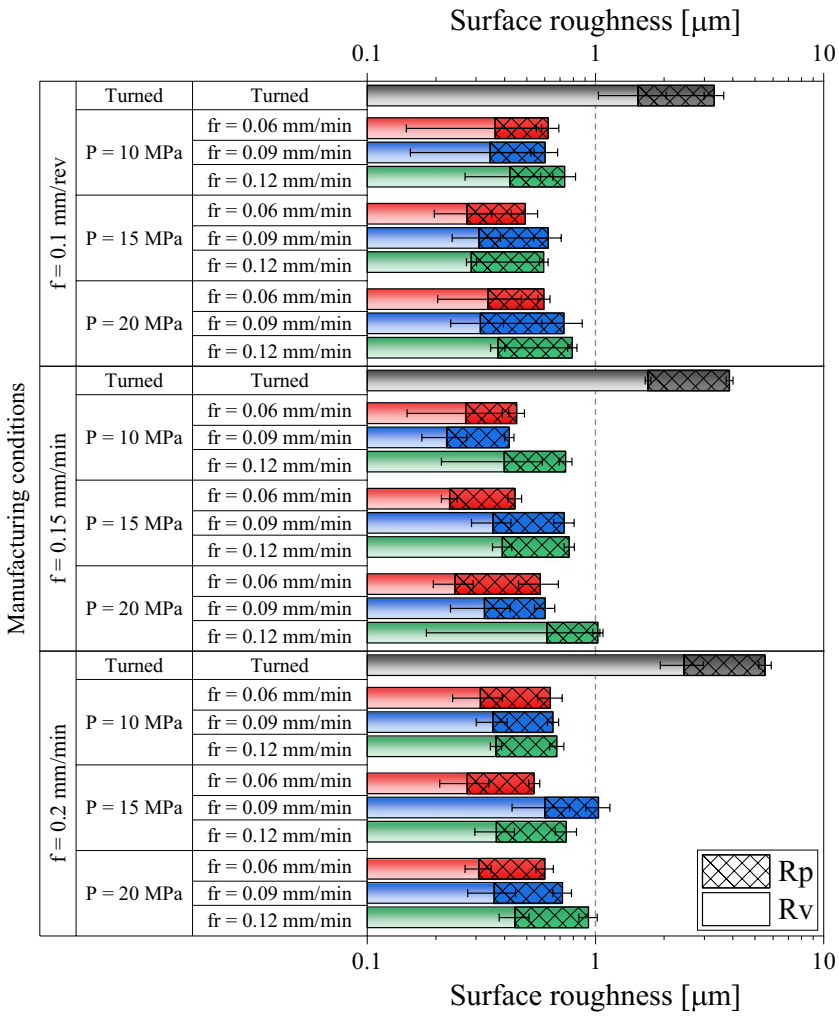

Fig. 5 Effect of the turning feed and deep rolling pressure and feed on the maximum profile peak height (Rp) and maximum profile valley depth (Rv) of hardened AISI 4140 steel

The effect of deep rolling pressure on Rp is presented on Fig. 6(c), where an increase in deep rolling pressure (P) and, therefore, in deep rolling force, promotes higher roughness amplitudes. Higher forces can deform the surface more easily and are capable of creating a new pattern with grooves. Considering the effect of the turning feed (f) on Rv, Fig. 6(d) indicates an increase in the roughness amplitude with the elevation of the turning feed, reducing the ability of deep rolling to achieve a smoother surface. Figure 6(e) shows an almost linear relationship between deep rolling feed (f_r) and Rv. An increase in the rolling feed decreases the overlap and, therefore, its intensity, reducing the surface deformation and promoting higher roughness amplitudes.

Figure 7 presents the interaction effect plot between deep rolling pressure (P) and deep rolling feed (f_r) for Rp. The effect of deep rolling feed (f_r) is more pronounced under higher deep rolling pressures. Deep rolling feed has an influence related to the alteration of the overlap, promoting higher roughness values for higher feeds [13]. Elevated deep rolling feeds generate a topography with grooves [10], which possess an effect on the surface roughness analogous to the turning tool nose radius. Combined with higher pressures, higher deep rolling feeds can promote more intense surface deformation and produce grooves that increase surface roughness (Fig. 7).

3.2 Surface topography and APSD analyses

The data concerned with the surface topography were used to generate the APSD spectra presented in Figs. 8, 9, 10, and 11. Figure 8 shows the APSD spectrum for the turned samples on its left and an image obtained through optical microscopy on the right. The first three peaks on Fig. 8 are related to the distinct turning feed values used. The feed values define the wavelength of the signal and the power spectrum indicates the values of the frequency (calculated as the inverse of feed). Figure 8 shows peaks related to each of the feeds used, in addition to lower peaks at higher frequencies. These lower peaks could be a consequence of the fact that the tool shape is not sinusoidal [16]. As observed on the right side of Fig. 8, the turned sample presents a series of marks. Some of them are easily seen and are directly related

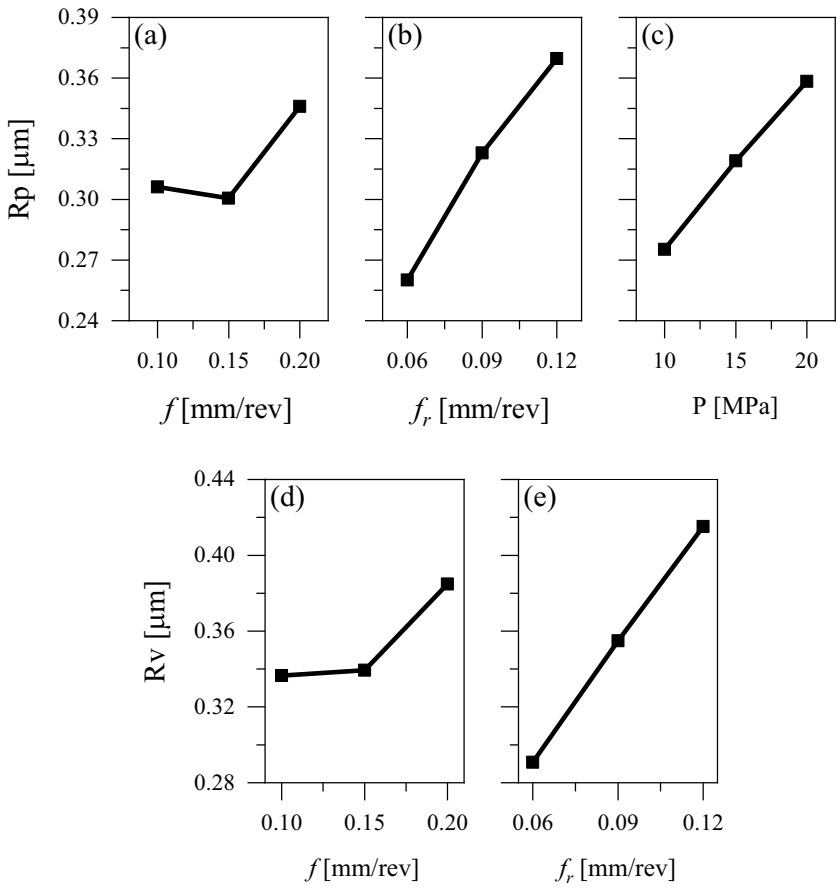

Fig. 6 Main effects plots for Rp: (**a**) turning feed, (**b**) deep rolling feed, (**c**) deep rolling pressure; main effects plots for Rv: (**d**) turning feed and (**e**) deep rolling feed

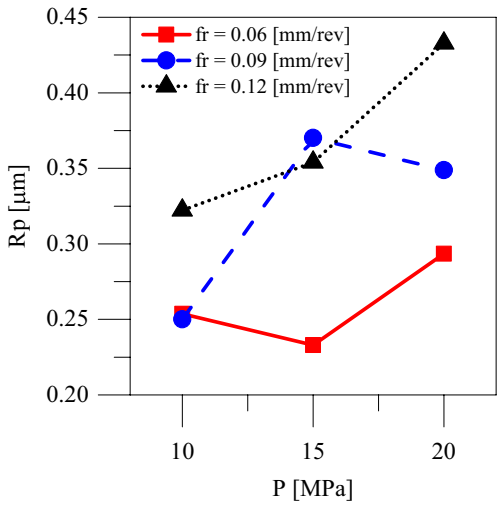

Fig. 7 Interaction effect plot for Rp

to the turning feed, but other marks can be observed. These marks are probably related to the surface deformation generated by the tool-surface and chip-surface contact and are responsible for the lower peaks seen at higher frequencies. The first peak shown in Fig. 8 presents higher amplitude and is related to the highest turning feed used (f = 0.20 mm/rev). In addition to the position of the peaks (related to the frequency resulting from the feed employed), the peaks' amplitude is also consistent with the turning feed values, i.e., the higher the feed, the higher the surface profile amplitude, and a higher peak on the APSD profile.

The spectrum resulting from the profiles generated for the samples deep rolled with a pressure of 10 MPa can be seen on the left side of Fig. 9, together with optical microscopy images of the surfaces on the right side. Peaks related to both deep rolling and previous turning feeds can be noted. Higher deep rolling feeds produce peaks with higher amplitude. For the lowest deep rolling feed (f_r = 0.06 mm/rev), the peaks related to the previous turning present a higher amplitude than the deep rolling peaks, behavior not observed for the other deep rolling feed values (f_r = 0.09 and 0.12 mm/rev). The APSD results obtained using the lowest deep rolling feed (top left of Fig. 9) present peaks with wavelength of 0.06 mm (spatial frequency of 16.667 mm^{-1}), which correspond to the deep rolling feed. However, a series of peaks that are not associated with the deep rolling process can be seen, e.g., peaks with spatial frequencies of 6.67 and 10 mm^{-1}, which correspond to the turning feeds of 0.15 and 0.10 mm/rev, respectively. The turning parameters are

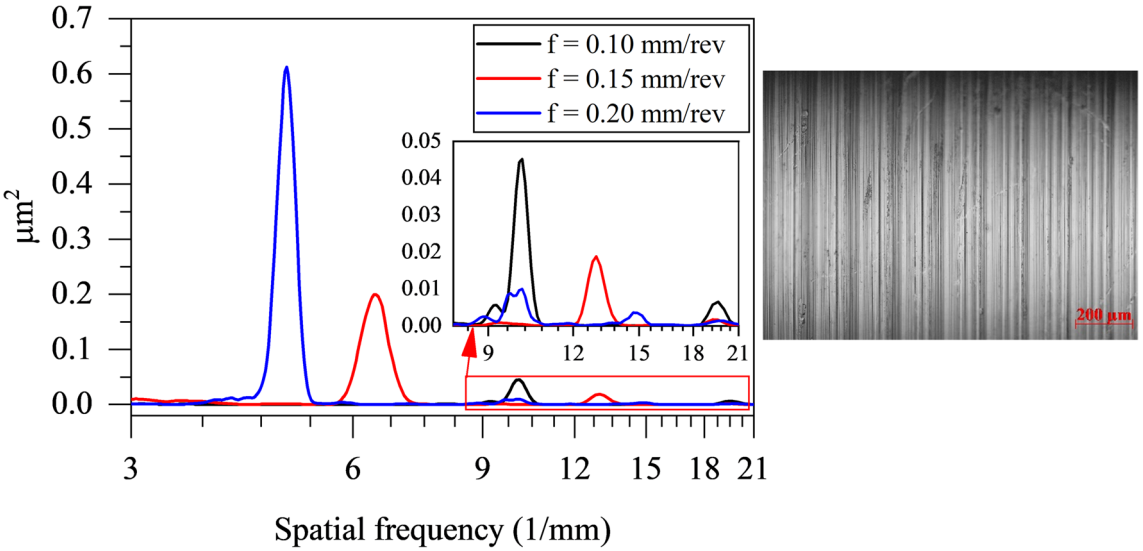

Fig. 8 Areal power spectral density analysis (left) and optical microscopy image (right) of a turned surface

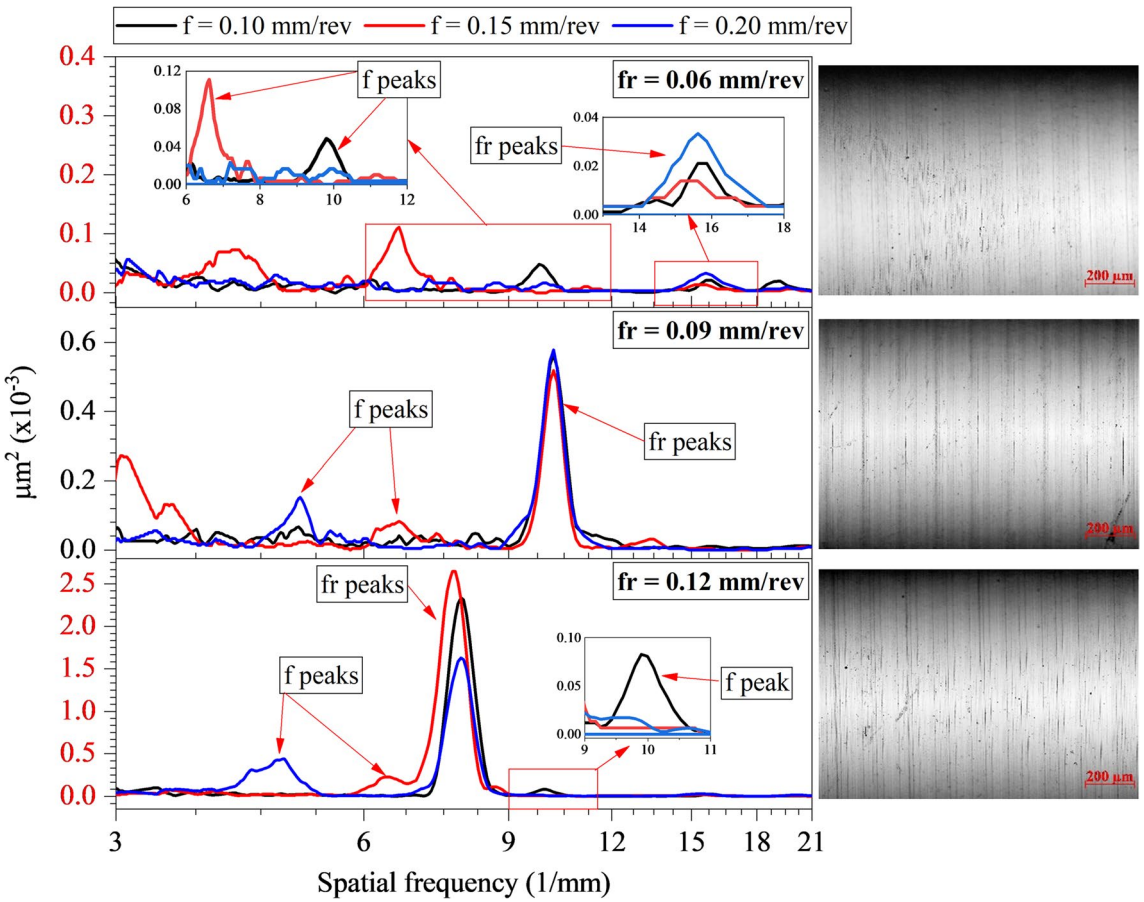

Fig. 9 Areal power spectral density analyses (left) and optical microscopy images of the corresponding surfaces (right) of samples deep rolled using $P = 10$ MPa

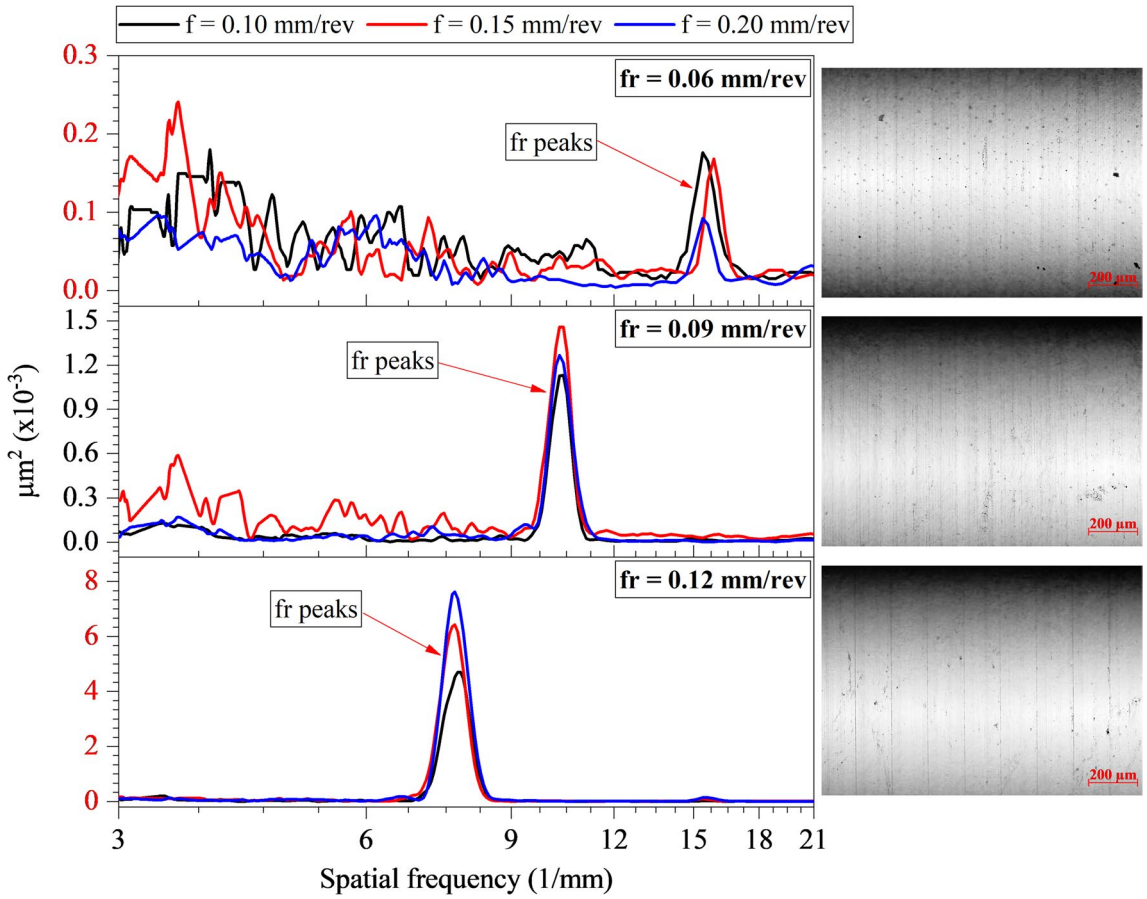

Fig. 10 Areal power spectral density analyses (left) and optical microscopy images of the corresponding surfaces (right) for samples deep rolled using $P = 15$ MPa

related to the surface marks observed on the right side of Fig. 9; however, they are less evident than those shown in Fig. 8. For the lowest and intermediate turning feed values ($f = 0.10$ and 0.15 mm/rev, respectively), turning feed peaks predominate over the deep rolling feed peaks. In contrast, for the highest turning feed of 0.2 mm/rev (5 mm^{-1}), the peak with a spatial frequency of 16.667 mm^{-1} (deep rolling feed) predominates. The other peaks produced under this condition are related to the surface deformation process. With an increase in the deep rolling feed, the peaks related to the previous turning operation had a lower amplitude in comparison to the deep rolling peaks, indicating the predominance of deep rolling on the surface characteristics.

With the increase in deep rolling pressure to 15 MPa (Fig. 10), the turning feed peaks presented in Fig. 9 can no longer be seen. An increase in pressure and, consequently, in the surface plastic strain severity, promotes a concentration of peaks associated with f_r, eliminating those resulting from the previous turning operation. The surface marks observed after turning and deep rolling employing the lowest pressure are not evident in Fig. 10 (right side). The elevation in the amplitude of the peaks generated by deep rolling indicate the process ability to generate a new pattern on the surface with the increase in pressure.

With a further increase in pressure (Fig. 11), the deep rolling peaks present the highest amplitude, especially for the intermediate and highest deep rolling feed values ($f_r = 0.09$ and 0.12 mm/rev, respectively). This behavior can be explained by the fact that elevating the deep rolling pressure increases the plastic strain severity. The lowest deep rolling feed ($f_r = 0.06$ mm/rev) generates a more random surface due to the lower distance between subsequent deep rolling paths, as can be observed on the top right side of Fig. 11 (a series of marks without a clear pattern and small cracks). The pressure of 15 MPa is able to eliminate the surface pattern produced during turning and, combined with the higher deep rolling feeds, increases the amplitude of the APSD peaks even further. Therefore, a new surface pattern is generated, with surface peaks presenting wavelength equivalent to the deep rolling feed (observed on the optical microscopy images on the right side of Fig. 11). This behavior was previously reported by Rodríguez et al. [10], who also noticed grooves on the deep rolled surface of AISI 1045 steel when high pressures (from 30 to 45 MPa) were applied.

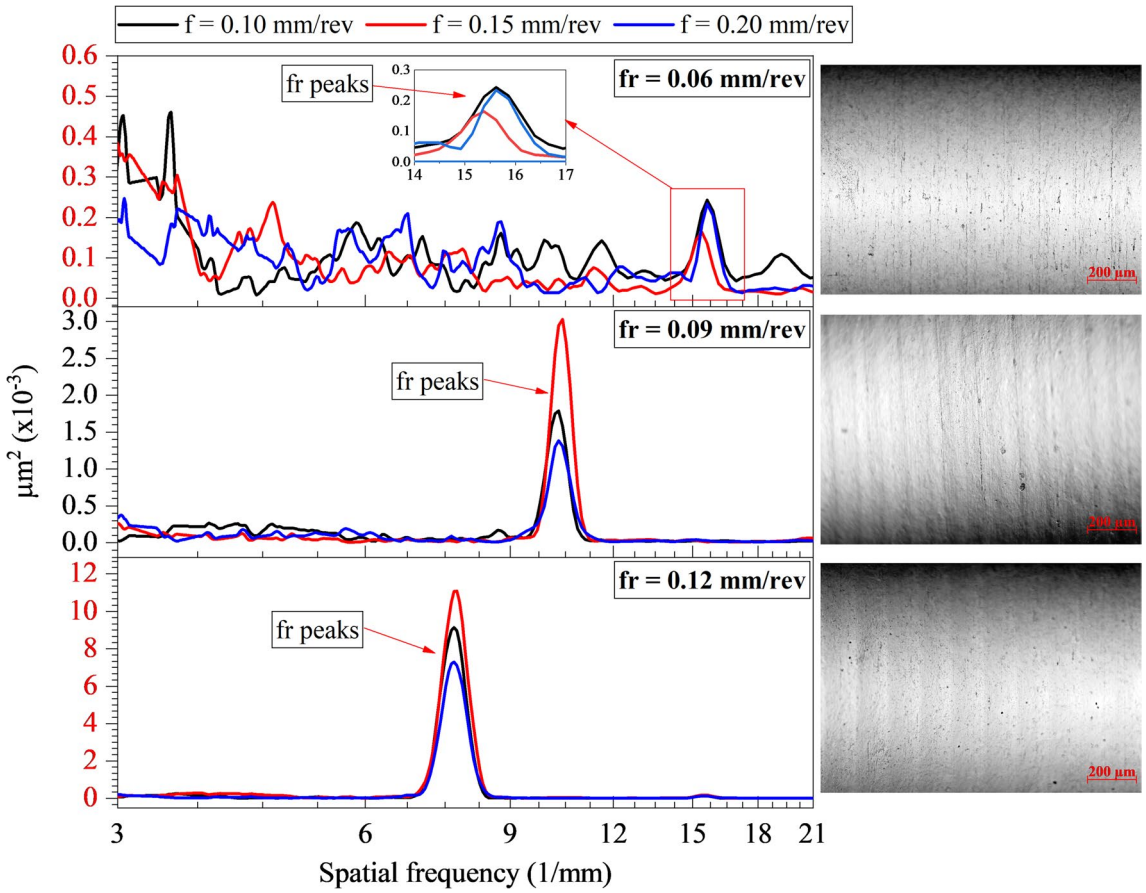

Fig. 11 Power spectral density analyses (left) and optical microscopy images of the corresponding surfaces (right) for samples deep rolled using $P = 20$ MPa

Using the lowest deep rolling feed, the distance between two subsequent paths is reduced. This condition induces a higher complexity on the surface deformation, creating a series of peaks with larger spatial distribution, as can be seen in the APSD analysis of the samples produced with a deep rolling feed of 0.06 mm/rev (Figs. 10 and 11). This trend was eliminated after deep rolling using a feed of 0.12 mm/rev.

3.3 Surface topography and surface texture directionality

The surface topography data were also used to generate the morphological roses presented in Figs. 12 and 13. The morphological rose allows the analysis of the isotropy/anisotropy of a surface. Figure 12 corresponds to the turned surface and indicates an oriented surface with the highest amplitude for 90°, followed by other directions of high amplitude for orientations near 90°, thus suggesting an anisotropic surface. Figure 13 presents the roses corresponding to the samples deep rolled under distinct conditions, where different morphologies can be seen (highest amplitude for 0°), especially when compared to the turned surface.

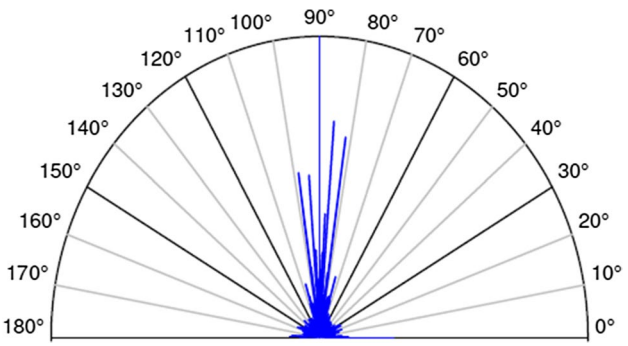

Fig. 12 Morphological rose for the turned sample

Different levels of the deep rolling parameters induce distinct morphological modifications. For the lowest deep rolling feed ($f_r = 0.06$ mm/rev), an increase in pressure promotes a loss of motifs directionality, indicating the tendency to produce a surface with isotropic characteristics, and reaching an approximately random surface under the highest deep rolling pressure ($P = 20$ MPa).

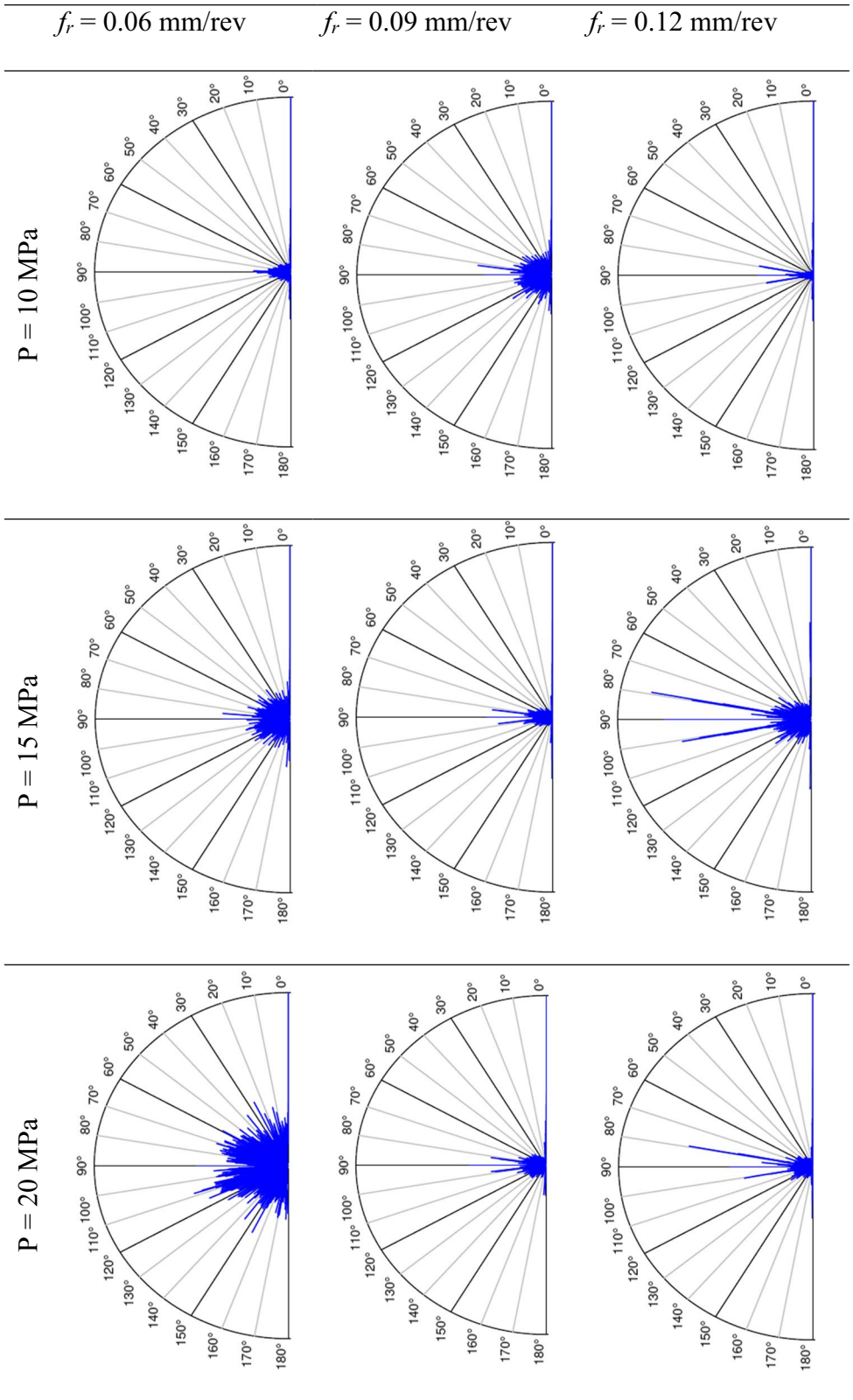

Fig. 13 Morphological roses: effect of deep rolling pressure and feed on the surface texture directionality

For the other deep rolling feed values, an increase in pressure (particularly from the lowest to the intermediate value) induces a more oriented surface. Considering the elevation of f_r for the same pressure, it can be seen that higher feeds induced a more oriented and anisotropic surface. This behavior indicates an interaction effect between *fr* and *P*.

The generation of an anisotropic surface after deep rolling with a single pass was reported by Oliveira et al. [21], who

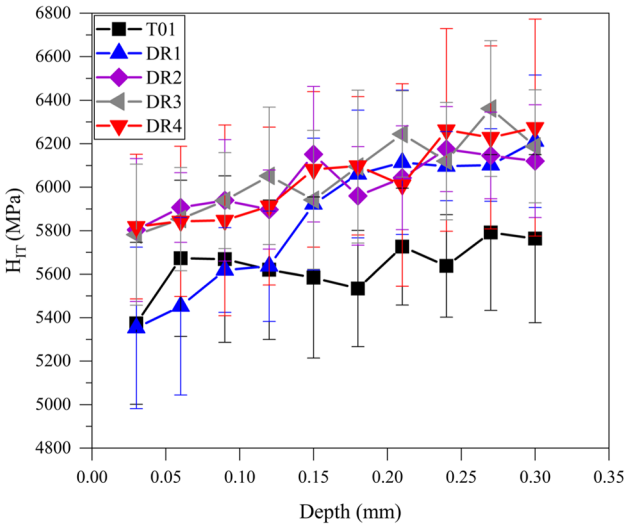

Fig. 14 Ultra-microhardness analysis of selected samples

noticed an increase on surface plastic strain with the elevation of the number of deep rolling passes, leading to a more isotropic surface. In the present work, the combination of low feed and high pressure increase the surface plastic strain, producing a less oriented (isotropic) surface. For higher deep rolling feeds and pressures, a new orientation is produced on the surface (anisotropic surface).

3.4 Microhardness and microstructure analyses

The ultra-microhardness values obtained are shown in Fig. 14 and correspond to the average of ten measurements. Firstly, one can observe that the turned sample (T01) presents the lowest mean hardness along the measured depth. The second lowest hardness is recorded for the sample turned with $f = 0.10$ mm/rev and deep rolled with $P = 10$ MPa (DR1) that indicates an increase on hardness on the subsurface. All the other samples (DR2: $f = 0.10$ mm/rev and $P = 20$ MPa; DR3: $f = 0.20$ mm/rev and $P = 10$ MPa; and DR4: $f = 0.20$ mm/rev and $P = 20$ MPa) presented almost the same hardness values; they present an increase on the subsurface hardness. Deep rolling was capable of increasing hardness regardless of the parameters used. The increase in subsurface hardness probably occurs because of the higher subsurface stresses generated by the Hertz contact [22]. These hardness results confirm the intense surface and subsurface deformation promoted by deep rolling.

The microstructure of the turned samples is presented in Fig. 15a ($f = 0.10$ mm/rev) and b ($f = 0.20$ mm/rev). Both samples present martensite on the surface and subsurface. For the turned samples, no distinction can be observed between the surface and subsurface regions, regardless of the turning feed used. Considering the deep rolled specimens (Fig. 15c, d), one can observe a deformation layer close to the surface (detail in Fig. 15c). This deformation was not on

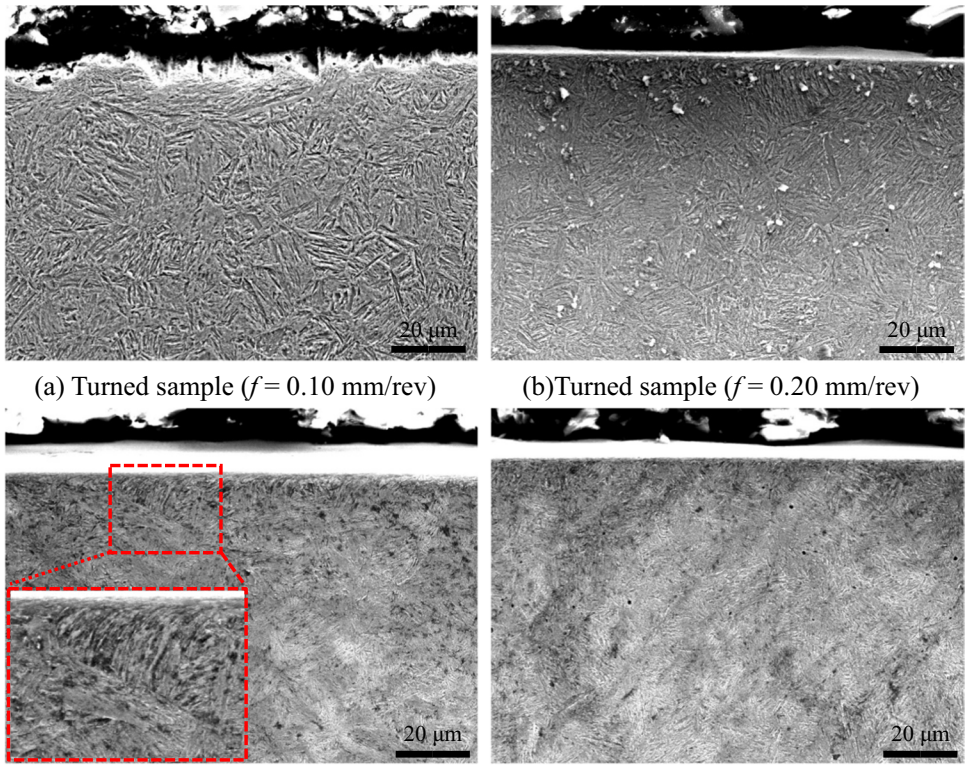

(a) Turned sample ($f = 0.10$ mm/rev) (b)Turned sample ($f = 0.20$ mm/rev)

(c) DR ($f = 0.10$ mm/rev; P = 20 MPa) (d) DR ($f = 0.20$ mm/rev; P = 20 MPa)

Fig. 15 Hardened AISI 4140 steel microstructure after (**a**) turning with $f = 0.10$ mm/rev, (**b**) turning with $f = 0.20$ mm/rev, (**c**) deep rolling with $f = 0.10$ mm/rev and $P = 20$ MPa, and (**d**) deep rolling with $f = 0.20$ mm/rev and $P = 20$ MPa

the turned samples and is caused by deep rolling, which is the responsible for the hardness increase recorded in Fig. 14. This surface deformation, which intensity is dependent on the deep rolling parameters, influences the surface texture patterns generated by the process, as seen on the APSD and morphological roses presented in Sects. 3.2 and 3.3, respectively.

3.5 Fatigue analysis

3.5.1 Number of cycles to failure

Figure 16 presents the results for fatigue life for each parameter combination. Regarding the turned samples, it can be seen that the highest turning feed promotes the lowest number of cycles to failure, probably because of the influence of the roughness profile on stress concentration. The lowest and intermediate feed values produced equivalent number of cycles to failure. In addition to roughness, the effect of residual stresses on the fatigue behavior must be taken into account. Increasing the turning feed could produce a more compressive residual stress state, thus offsetting its deleterious influence on surface roughness (stress concentration) and leading to a similar number of cycles under fatigue. This behavior was described by Lopes et al. [23], who reported the same fatigue limit after turning AISI 4140 steel with two distinct feeds (0.12 and 0.18 mm/rev).

The increase in the intensity of the compressive residual stresses with the elevation of the turning feed was observed by Javidi et al. [24] when turning 34CrNiMo6 steel. Similarly, an increase in the intensity of the compressive residual stresses beneath the surface with the elevation of feed when turning AISI 52100 bearing steel was reported by Dahlman et al. [25].

Considering the deep rolled samples, one can notice the ability of deep rolling to increase the fatigue life (regardless of alterations on the manufacturing parameters). In general, the combination of higher deep rolling feeds and pressures promotes longer fatigue life. Moreover, an increase in the number of cycles to failure can be observed after deep rolling the samples turned using the highest feed. The increase in fatigue life after deep rolling has been previously observed and according to Avilés et al. [7], the main reason behind the fatigue life increase is the inducement of

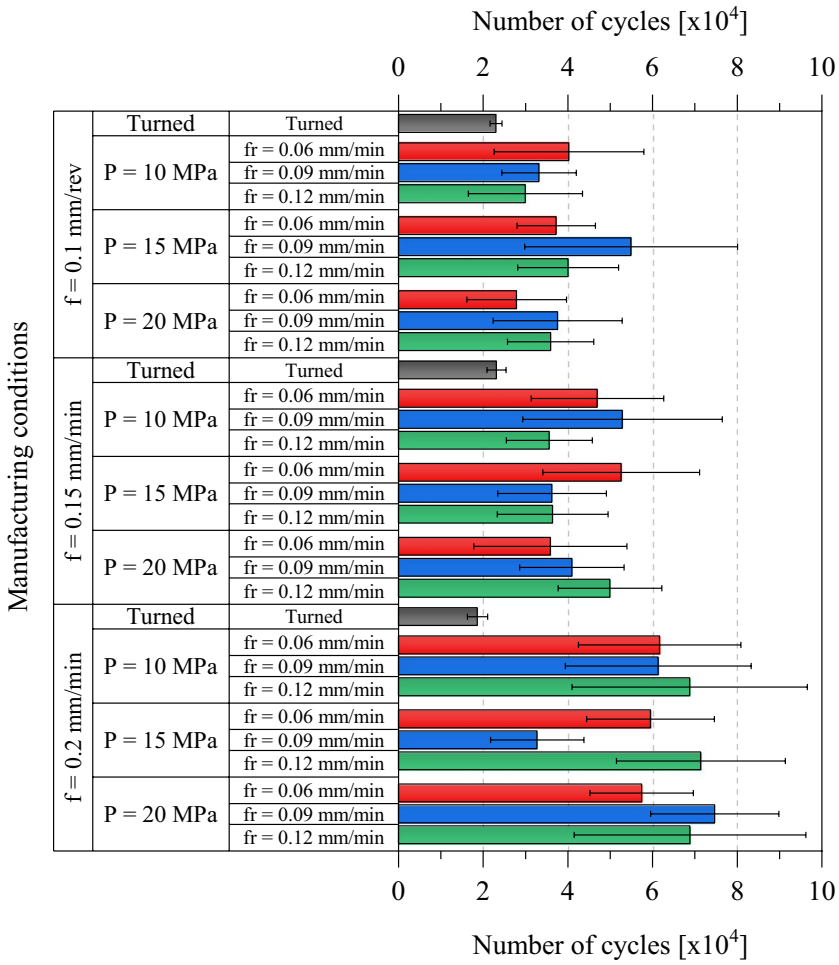

Fig. 16 Influence of turning feed, deep rolling feed, and deep rolling pressure on the number of cycles to failure of hardened AISI 4140 steel

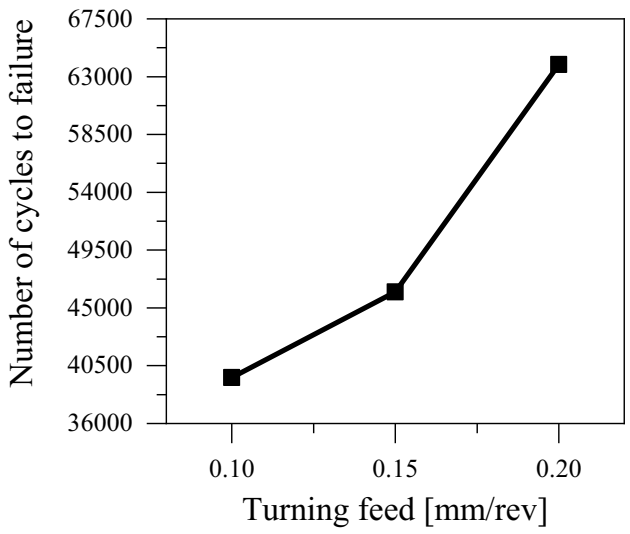

Fig. 17 Effect of turning feed on the number of cycles to failure of the deep rolling hardened AISI 4140 steel

compressive residual stresses by deep rolling. Martins et al. [9] and Prabhu et al. [5] observed an increase in the fatigue life of AISI 4140 steel after deep rolling, and stated that the reduction in roughness [9] and the inducement of compressive residual stresses [5] as the main reasons for the fatigue life increase. The deep rolling process was able to increase the fatigue resistance. Deep rolling promoted a surface and subsurface hardening that were identified by microstructure changes and ultra-microhardness measurements; these alterations can influence the fatigue resistance by altering the crack propagation rates.

In addition to the evaluation of roughness amplitude and the fatigue life analysis, the present work also conducted APSD and directionality analyses. These two analyses were able to identify distinct behaviors with the increase in deep rolling pressure for different deep rolling feeds and the same trend is repeated for the fatigue life results. For the lowest deep rolling feed ($fr = 0.06$ mm/rev), an increase in pressure promotes a decrease in fatigue life and the generation of a less oriented morphology, probably because of the generation of surface defects. When considering the APSD spectrum, the pressure rise (for $fr = 0.06$ mm/rev) does not increase the amplitude of the *fr* related peaks to one order of magnitude higher than the rest of the spectrum. For the other deep rolling feeds (0.09 and 0.12 mm/rev), the fatigue life reduction under higher deep rolling pressure values is not always observed. Furthermore, the morphological roses are more oriented for higher deep rolling pressures. Considering the APSD spectra, the *fr*-related peaks always present higher amplitudes than the rest of the spectrum, and this difference increases with pressure. Therefore, the APSD and surface texture directionality analyses are able to identify surface modifications that probably present a significant influence on the fatigue behavior.

Other likely relationship between APSD and the number of cycles to fatigue fracture is the fact that the condition responsible for higher number of cycles presents higher peaks related to the deep rolling feed, in addition considerable peaks' amplitude at other apparently random frequencies in the spectrum. Thus, a less oriented and more random surface allows a higher number of cycles until failure. However, this less oriented surface is only beneficial for the conditions that do not introduce surface defects. The existence of a high only peak on the APSD spectrum could indicate a profile with an oriented topography that could still act as a stress concentrator.

An analysis of variance (significance level of 0.05) was conducted for the fatigue results and the only factor statistically significant is turning feed (main effect plot shown in Fig. 17). An increase in turning feed results in longer fatigue lives for the deep rolled samples. Although the surface produced using higher turning feed values presents peaks with higher amplitude, the deformation of these peaks by deep rolling could generate more compressive residual stresses that led to longer fatigue lives. Even considering that the roughness values obtained after deep rolling with higher *f* values are statistically higher, all the deep rolled specimens presented low roughness values (especially in comparison with the turned samples), reducing stress concentration in the topography.

3.5.2 Fatigue fracture analysis

The cross-section of selected fractured specimens can be seen in Fig. 18. The main difference between the only turned and turned plus deep rolled samples is the presence of ratchet marks in the former. The ratchet marks are generated when two fractures that are nucleated at distinct regions reach each other after propagation. One of the conditions that can promote this behavior is stress concentration. Therefore, the roughness profile of the turned samples acted as a stress concentrator, increasing the number of nucleation regions. In contrast, deep rolling reduces the number of crack nucleation sites, as reported by Muñoz-Cubillos et al. [2] after analyzing the fatigue fractures of austenitic stainless steels, and Martins et al. [9] after studying the fractures on AISI 4140 low alloy steel.

For the sake of a better understanding of the fatigue phenomenon, details of the fractured cross-sections were analyzed in the search for the regions of crack nucleation and final fracture (Fig. 19(a)). The final fracture regions can be identified by the presence of dimples (Fig. 19(b)). The presence of dimples indicates a final overload fracture with ductile characteristics [7]. Besides the final overload region, other characteristics can be identified. Figure 19(c) shows

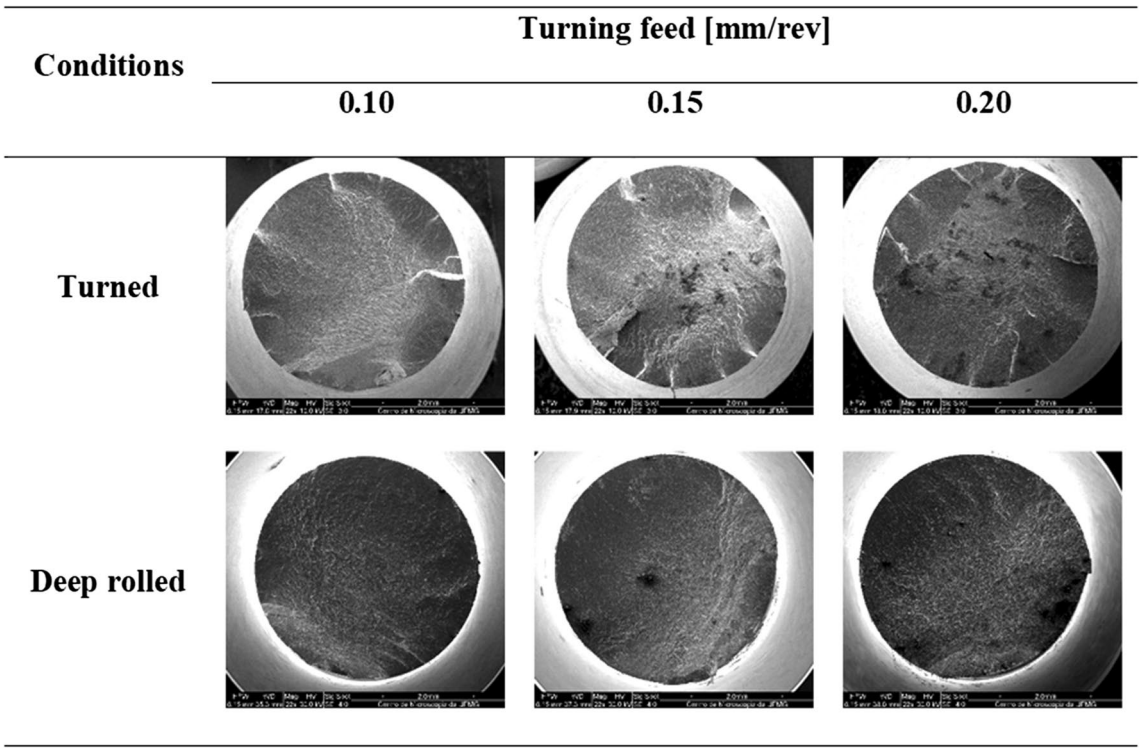

Fig. 18 Fatigue fractures for distinct manufacturing conditions (deep rolling at $f_r = 0.06$ mm/rev and $P = 15$ MPa)

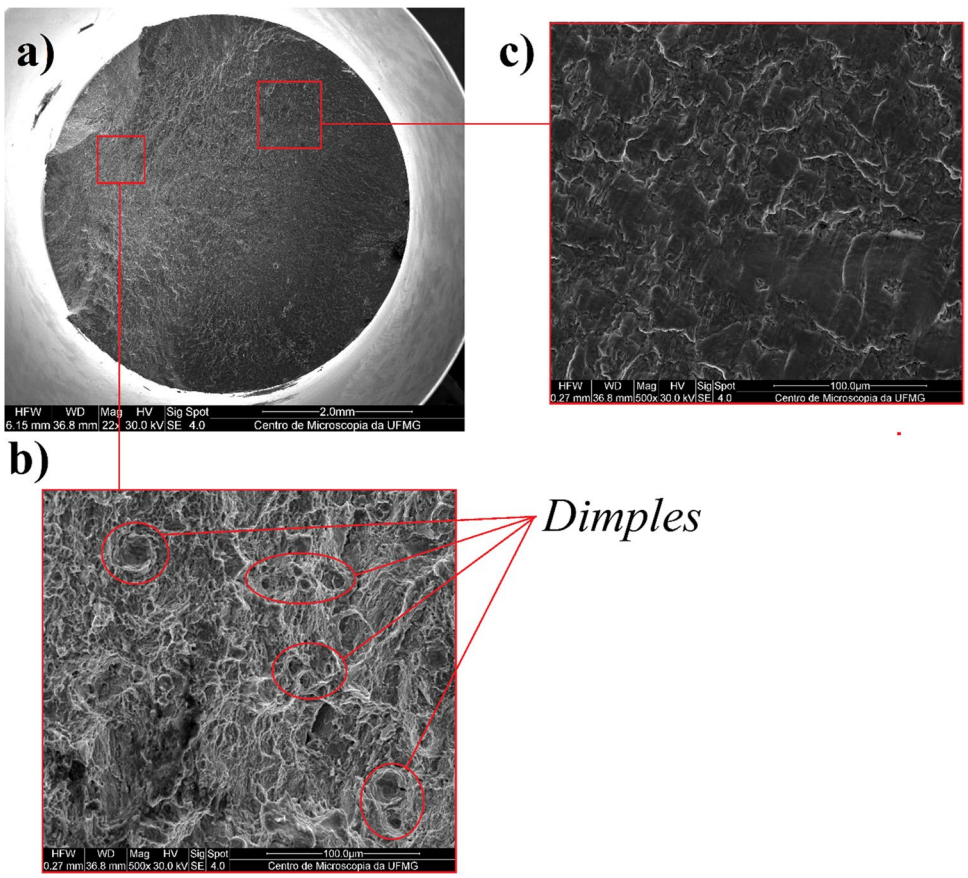

Fig. 19 Fractured deep rolled sample ($fr = 0.12$ mm/rev and P = 15 MPa): (**a**) cross-section, (**b**) region of final overload with dimples, and (**c**) region of crack propagation

diagonal lines (striations) associated with crack propagation. These features (dimples and striations) suggest that the fatigue fracture began beneath the surface, because of the superficial deformation as indicated on Fig. 15, and probably as a consequence of the compressive residual stresses induced near the surface by deep rolling. The fracture propagates towards the surface, where the final fracture happens. In contrast, the turned samples possesses numerous regions of crack nucleation near the surface and a final fracture close to the center of the sample cross-section.

4 Discussion

Turned and deep rolled surfaces present a series of differences. The surface roughness of the turned samples presents a quadratic relationship with feed (*f*) together with a highly oriented (anisotropic) surface with lower hardness. The specimens with these characteristics are not capable to withstand an elevated number of cycles before fracture, thus indicating surface characteristics that can be detrimental to the fatigue strength of the material.

In contrast, the deep rolled surfaces present lower roughness, a more random (isotropic) orientation, higher hardness, and distinct peaks on the APSD spectrum. Moreover, microstructure deformation is evident in the deep rolled specimens. The abovementioned characteristics are probably responsible for the observed increase in fatigue life. Deep rolling is also effective in inducing compressive residual stresses of higher intensity, which can further increase the fatigue life of the investigated material by reducing the crack propagation rate, thus elevating the number of cycles to failure.

5 Conclusions

After producing fatigue specimens on hardened AISI 4140 steel (40 HRC) by means of turning alone and turning followed by deep rolling, the surface topography, hardness, and microstructure of the specimens were analyzed. The following conclusions can be drawn:

- Deep rolling was able to reduce the surface roughness for all factor combinations used; however, excessively high deep rolling pressure and feed promoted an increase in surface roughness.
- The influence of turning feed on surface roughness was detected after deep rolling, i.e., an increase in turning feed generates a rougher surface that is harder to deform, impairing the reduction in roughness by deep rolling.
- Deep rolling affected the ratio of the Rp to the Rv roughness parameters, increasing the contribution of Rv to Rz.
- The areal power spectral density (APSD) analysis allowed to identify new surface characteristics introduced by deep rolling, in addition to observing the predominance of deep rolling in relation to turning from a determined pressure level (15 MPa). Such behavior cannot be clearly observed employing the traditional roughness parameters.
- The morphological rose analysis allowed to establish that the lowest deep rolling feed generated a more random (isotropic) surface. Moreover, deep rolling with the highest feed and pressure values altered the surface orientation, which became more anisotropic.
- The rolling action of the deep rolling tool was capable to deform the surface and increase surface and subsurface hardness, also promoting microstructure deformation that can increase the fatigue strength by promoting higher surface hardness and smaller grain.
- Regarding the fatigue behavior, deep rolling increases the fatigue life, regardless of the parameters used, due to the reduction in roughness, microstructure deformation, and the likely induction of compressive residual stresses. Surprisingly, the influence of the turning feed was more significant on fatigue life than that of the deep rolling parameters. More specifically, longer fatigue lives were obtained after deep rolling the samples that were turned using the highest feed (and presented higher roughness after turning), probably due to more intense surface compressive residual stresses.
- Deep rolling altered the features of the fatigue fracture, reducing the number of nucleation sites and changing the position of the final fracture region.
- The optimal parameters combination is turning with a feed of 0.20 mm/rev, followed by deep rolling with a feed of 0.09 mm/rev and a pressure of 20 MPa. This condition produced the lowest surface roughness, was capable of eliminating the influence of turning on the APSD spectrum, and represented the longest mean fatigue life.

Funding The authors acknowledge the financial support provided by the Coordination for the Improvement of Higher Education Personnel-Brazil (CAPES) under Code 001.

Data availability Not applicable.

Code availability Not applicable.

Declarations

Ethics approval Not applicable.

Consent to participate Not applicable.

Consent for publication The authors give full consent to the publisher for the publication of this work.

Competing interests The authors declare no competing interests.

References

1. Bannantine JA, Comer JJ, Handrock JL (1989) Fundamentals of metal fatigue analysis. Prentice Hall, Englewood Cliffs (ISBN: 978-0133401912)
2. Muñoz-Cubillos J, Coronado JJ, Rodríguez SA (2017) Deep rolling effect on fatigue behavior of austenitic stainless steels. Int J Fatigue 95:120–131. https://doi.org/10.1016/j.ijfatigue.2016.10.008
3. Hassani-Gangaraj SM, Carboni M, Guagliano M (2015) Finite element approach toward an advanced understanding of deep rolling induced residual stresses, and an application to railway axles. Mater Des 83:689–703. https://doi.org/10.1016/j.matdes.2015.06.026
4. Altenberger I (2005) Deep rolling—the past, the present and the future. In: Schulze V, Niku-Lari A (eds) Proceedings of 9th International Conference on Shot Peening. Paris, France. IITT-International, pp 144–155
5. Prabhu PR, Kulkarni SM, Sharma S (2020) Multi-response optimization of the turn-assisted deep cold rolling process parameters for enhanced surface characteristics and residual stress of AISI 4140 steel shafts. J Market Res 9(5):11402–11423. https://doi.org/10.1016/j.jmrt.2020.08.025
6. Nalla RK, Altenberger I, Noster U, Liu GY, Scholtes B, Ritchie RO (2003) On the influence of mechanical surface treatments -deep rolling and laser shock peening on the fatigue behavior of Ti-6Al-V at ambient and elevated temperatures. Mater Sci Eng A 355:216–230. https://doi.org/10.1016/S0921-5093(03)00069-8
7. Avilés R, Albizuri J, Rodríguez A, López De Lacalle LN (2013) Influence of low-plasticity ball burnishing on the high-cycle fatigue strength of medium carbon AISI 1045 steel. Int J Fatigue 55:230–244. https://doi.org/10.1016/j.ijfatigue.2013.06.024
8. Prabhu PR, Kulkarni SM, Sharma SS, Jagannath K (2014) Surface layer alterations in AISI 4140 steel from turn-assisted deep cold rolling process. Int J Mech Eng Technol 5(9):245–250
9. Martins AM, Rodrigues PCM, Abrão AM (2022) Influence of machining parameters and deep rolling on the fatigue life of AISI 4140 steel. Int J Adv Manuf Technol 121:6153–6167. https://doi.org/10.1007/s00170-022-09703-1
10. Rodríguez A, López De Lacalle LN, Celaya A, Fernández A, Lamikiz A (2011) Ball burnishing application for finishing sculptured surfaces in multi-axis machines. Int J Mechatron Manuf Syst 4(3/4):220–237. https://doi.org/10.1504/IJMMS.2011.041470
11. Klocke F, Liermann J (1998) Roller burnishing of hard turned surfaces. Int J Mach Tools Manuf 38:419–423. https://doi.org/10.1016/S0890-6955(97)00085-0
12. Majzoobi GH, Jouneghani FZ, Khademi E (2016) Experimental and numerical studies on the effect of deep rolling on bending fretting fatigue resistance of Al7075. Int J Adv Manuf Technol 82:2137–2148. https://doi.org/10.1007/s00170-015-7542-z
13. Némat M, Lyons AC (2000) An investigation of the surface topography of ball burnished mild steel and aluminium. Int J Adv Manuf Technol 16:469–473
14. Denkena B, Abrão A, Kroedel A, Meyer K (2020) Analytic roughness prediction by deep rolling. Prod Eng Res Devel 14:345–354
15. Asmaa TM, Kesba MM, Abu-gharbia F (2019) Ball burnishing of internal turned surfaces. J Egypt Soc Tribol 16(1):33–43
16. Whitehouse D (2002) Surfaces and their measurement. Hermes Penton Science, London (ISBN: 9781903996010)
17. Zahouani H, Assoul M, Vargiolu R, Mathia T (2001) The morphological tree transform of surface motifs. Incidence in tribology. Int J Mach Tools Manuf 41:1961–1979. https://doi.org/10.1016/S0890-6955(01)00061-X
18. American Society of Mechanical Engineers (2010) Surface texture: (surface roughness, waviness, and lay): ASME B46. 1-2009. American Society of Mechanical Engineers
19. Lee WK, Ratnam MM, Ahmad ZA (2017) Detection of chipping in ceramic cutting inserts from workpiece profile during turning using fast Fourier transform (FFT) and continuous wavelet transform (CWT). Precis Eng 47:406–423. https://doi.org/10.1016/j.precisioneng.2016.09.014
20. Grzesik W, Żak K, Kiszka P (2014) Comparison of surface textures generated in hard turning and grinding operations. Procedia CIRP 13:84–89. https://doi.org/10.1016/j.procir.2014.04.015
21. Oliveira DA, Martins AM, Magalhães FC, Abrão AM (2022) Characterization of the topography generated by low plasticity burnishing using advanced techniques. Surf Coat Technol. 448:128891. https://doi.org/10.1016/j.surfcoat.2022.128891
22. Hertz H (1882) Ueber die berührung fester elastischer körper. Journal für die reine und angewandte Mathematik (Crelles Journal) 1882(92):156–171. https://doi.org/10.1515/crll.1882.92.156
23. Lopes KSS, Sales WF, Palma ES (2008) Influence of machining parameters on fatigue endurance limit of AISI 4140 steel. J Braz Soc Mech Sci Eng 30(1):77–83. https://doi.org/10.1590/S1678-58782008000100011
24. Javidi A, Rieger U, Eichlseder W (2008) The effect of machining on the surface integrity and fatigue life. Int J Fatigue 30:2050–2055. https://doi.org/10.1016/j.ijfatigue.2008.01.005
25. Dahlman P, Gunnberg F, Jacobson M (2004) The influence of rake angle, cutting feed and cutting depth on residual stresses in hard turning. J Mater Process Technol 147(2):181–184. https://doi.org/10.1016/j.jmatprotec.2003.12.014